

## Detection of seizure rhythmicity by recurrences

Mary Ann F. Harrison,<sup>1,a)</sup> Mark G. Frei,<sup>2,b)</sup> and Ivan Osorio<sup>2,3,c)</sup>

<sup>1</sup>WVHTC Foundation, 1000 Technology Drive, Suite 1000, Fairmont, West Virginia 26554, USA

<sup>2</sup>Flint Hills Scientific L.L.C., 5040 Bob Billings Parkway, Suite A, Lawrence, Kansas 66049, USA

<sup>3</sup>Department of Neurology, University of Kansas Medical Center, 3901 Rainbow Blvd., Kansas City, Kansas 66160, USA

(Received 5 September 2007; accepted 29 July 2008; published online 26 August 2008)

Epileptic seizures show a certain degree of rhythmicity, a feature of heuristic and practical interest. In this paper, we introduce a simple model of this type of behavior, and suggest a measure for detecting and quantifying it. To evaluate our method, we develop a set of test segments that incorporate rhythmicity features, and present results from the application of this measure to test segments. We then analyze electrocorticogram segments containing seizures, and present two examples. Finally, we discuss the similarity of our method to techniques for detecting unstable periodic orbits in chaotic time series. © 2008 American Institute of Physics. [DOI: 10.1063/1.2973817]

**Epilepsy is the second most common neurological disorder, second only to stroke. Epileptic seizures often occur without warning, may be associated with loss of consciousness and violent tremors, and significantly degrade quality of life for those suffering from epilepsy. The brain activity that gives rise to seizures can be monitored through electrodes on the scalp or in direct contact with the brain. This activity shows certain patient-specific stereotypical features, which may be detectable before the onset of behavioral manifestations, and this activity frequently appears more “rhythmic” than background brain activity. These rhythmic signals frequently consist of repetitions of similar waveform patterns. In this paper, we describe a technique for detecting this type of rhythmic signal, which is derived from a time series analysis method for detecting unstable periodic orbits. Accurate detection of rhythmic signals, a subset of the vast variety of anomalous waveforms associated with epilepsy, may provide valuable information to benefit and improve implantable medical devices being developed to detect and disrupt epileptic signals.**

### I. INTRODUCTION

In the United States, epileptic seizures affect about 1% of the entire population. The abnormal brain activity associated with seizures can be monitored via scalp (EEG) or intracranial electrodes (ECoG). At present, EEG and/or ECoG are the main window through which the dynamics of epilepsy can be studied. Analysis of EEG and ECoG is thus of fundamental importance for understanding epilepsy and seizures.

Epileptic electrical activity originating from the same brain region has certain stereotypical features. Trains of nearly periodic spikes with similar morphology, spectrum,

and amplitude herald the nearness of a seizure. Variable duration wave bursts, composed of frequencies varying from approximately 5 to 45 Hz, are seen consistently at the same time from seizure onset and originating from the same site for a given patient. Sets or trains of monomorphic waves (i.e., with the same general shape) are referred to as being rhythmic and are frequently observed in such seizures. The duration of these wave patterns and their onset time in relation to electrographic seizure onset is relatively constant across seizures. Rhythmicity is a term widely used in electroencephalography as a qualitative description of repetitive waveform patterns, but one that lacks formal definition. While measures based on power spectral density may be useful for identifying the dominant frequencies present in a signal, the temporal organization of signal patterns and their morphology are not captured by these methods. In this paper, we focus on the development of techniques specifically geared towards a time domain pattern matching strategy to detect and quantify ECoG rhythmicities before, during, and after epileptic seizures.

Figure 1 illustrates the limitation of power spectral density (PSD) methods for detection of rhythmic patterns within ECoG signals. The signal in Fig. 1(a) is a simulated signal resembling an epileptiform pattern frequently observed preceding or during seizure events. We construct a signal with identical PSD by taking the Fourier transform of the original signal, randomly shuffling the phases, and inverse transforming back into the time domain. This same procedure is commonly used in nonlinear signal processing to determine whether the results of a nonlinear dynamical measure are due to a signal's time-frequency-energy properties or are really detecting nonlinear behavior.<sup>1</sup> We see from Fig. 1(b) that the rhythmic pattern has been destroyed. PSD-based methods will generate the same results for the two signals, yet we can visually detect qualitative differences in the two. Time domain statistics looking for repetitions of identical or similar wave shapes are useful for detecting the type of repetitive patterns depicted in Fig. 1(a).

<sup>a)</sup>Electronic mail: mharrison@wvhtf.org.

<sup>b)</sup>Author to whom correspondence should be addressed. Electronic mail: frei@fhs.lawrence.ks.us.

<sup>c)</sup>Electronic mail: iosorio@kumc.edu.

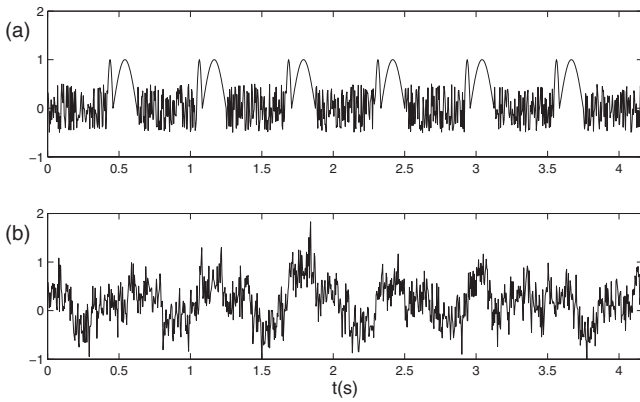


FIG. 1. (a) A simulated ECoG segment containing a frequently observed simulated spike-wave-type pattern commonly found in epileptiform ECoG. The repetitive waveform consists of a short spike followed by a longer half-wave, and may occur in unbroken trains or interspersed with arbitrary signal. The latter is the case in this segment, with the nonepileptiform arbitrary signal approximated by random noise. (b) A signal with the same power spectral density (PSD) as the signal depicted in (a), but with randomized phases. While the PSD is the same, the signal no longer shows the same type of rhythmic pattern as depicted in (a). However, time domain analysis methods based on signal recurrences can distinguish between these two signals.

Eckmann *et al.*<sup>2</sup> first introduced a technique of graphically depicting points which reoccur in a signal within a given tolerance, in order to uncover patterns in experimental data. This recurrence plot has led to the emergence of methods to identify and quantify repetitive patterns in time series based on similar techniques. These recurrence-based methods of signal analysis have been used to compute nonlinear dynamical properties of signals,<sup>3</sup> quantify nonstationarity,<sup>3-9</sup> detect unstable periodic orbits (UPOs),<sup>10-14</sup> estimate dynamical invariants,<sup>15,16</sup> and measure levels of synchrony.<sup>8,17</sup> Other statistics quantifying visually apparent structures in the recurrence plots, such as, the lengths of diagonal or horizontal lines, have been used to measure percent recurrence and percent determinism,<sup>4,18</sup> but the relationship between these statistics and features derived from visual inspection of the original signal is often unclear.<sup>19</sup> It is also not known if any of these statistics uncover new dynamical information, or are simply reflective of time-frequency-energy signal changes, as is likely the case with correlation dimension and Lyapunov exponent.<sup>20-24</sup>

In this paper, we develop and apply statistics based on recurrences that specifically relate to rhythmicity, a phenomenon of interest for seizure analysis. Specifically, we focus on the development of techniques geared towards a time domain pattern matching strategy to detect and quantify ECoG rhythmicities before, during, and after epileptic seizures. The organization of this paper is as follows. First, we define recurrence and illustrate typical recurrences seen in pre-seizure, seizure, and postseizure ECoG data. We then propose an operational definition of rhythmicity, and construct test signals that incorporate the necessary features of this definition. We describe our signal analysis technique, and demonstrate the technique on these test signals. We then present results from the application of the technique to ECoG segments containing epileptic seizures and discuss the results.

## II. RECURRENCES IN ECOG

The recurrence plot is typically defined in terms of the underlying metric used in computation of the correlation sum,<sup>25</sup>

$$R_{ij} = \Theta[\epsilon - \|(\mathbf{x}_i - \mathbf{x}_j)\|], \quad (1)$$

where  $R_{ij}$  is the recurrence between time series points  $\mathbf{x}_i$  and  $\mathbf{x}_j$ ,  $\epsilon$  is a length scale parameter, and  $\Theta$  is the Heaviside step function defined as the following:  $\Theta(z)=0$  if  $z<0$  and  $\Theta(z)=1$  if  $z>0$ . [By convention,  $\Theta(z=0)$  usually is defined as  $1/2$ , but here we define it as  $1$ .] The fraction of point pairs that are recurrent over the time series is the correlation sum (this has also been termed the recurrence rate<sup>26</sup>), and if there exists a power law scaling with  $\epsilon$  over at least a decade, then the exponent gives the correlation dimension ( $D_2$ ).<sup>25</sup>

The recurrence plot may be computed on scalar time series data in order to obtain a visual representation of the behavior by plotting  $R_{ij}$  as a function of data index  $i$  and time lag  $j$ . This method was originally designed to be used for graphical display of nonstationarity.<sup>2</sup> An unthresholded recurrence matrix (also called a global recurrence matrix or distance plot),<sup>27</sup>

$$R_{ij}^s = \|\mathbf{x}_i - \mathbf{x}_j\|, \quad (2)$$

indicates the minimum value of  $\epsilon$  required for a point pair to be recurrent.

We analyzed ECoG data from patients with pharmacoresistant epilepsy who underwent invasive evaluation for epilepsy surgery at the University of Kansas Comprehensive Epilepsy Center. The majority of the data was recorded using Ad-Tech depth electrodes, implanted stereotaxically into the amygdalo-hippocampal regions or extratemporally, while some data were recorded using subdural strip and grid electrodes. Most recordings contain 64 channels of data. Correctness of placement in all cases was assessed with MRI. Signals were amplified and digitized at 240 Hz with 10 bits of precision and  $0.59 \mu\text{V}/\text{bit}$ , using commercially available devices (Nicolet in Madison, WI). An automated seizure detection algorithm<sup>28</sup> was applied to the data to provide electrographic seizure onsets and to identify subclinical or clinical seizures missed during the monitoring period. Seizure identification and seizure onset scoring were confirmed through expert visual analysis by one or more epileptologists.<sup>28</sup>

Figure 2 shows recurrence plots for six single channel ECoG segments of 1000 points in length, approximately 4.17 s at a sampling rate of 239.75 Hz.<sup>29</sup> For all panels, the recurrence between scalar data points  $x_i$  and  $x_j$  were computed with  $\epsilon=0.03$ , or approximately 8% of the maximum amplitude for an entire length of a 9 min segment containing a seizure. Because recurrence plots are symmetric by definition, we compute only positive lags, which in Fig. 2 correspond to the upper triangle of each square recurrence panel. Figure 2(a) shows a segment of nonseizure ECoG (top) and its corresponding recurrence plot (bottom). Similarly, panels (b-f) show ECoG and the corresponding recurrence plots for precursor spiking (b), seizure onset (c), rhythmic seizure activity (d) and (e), and postseizure activity (f).

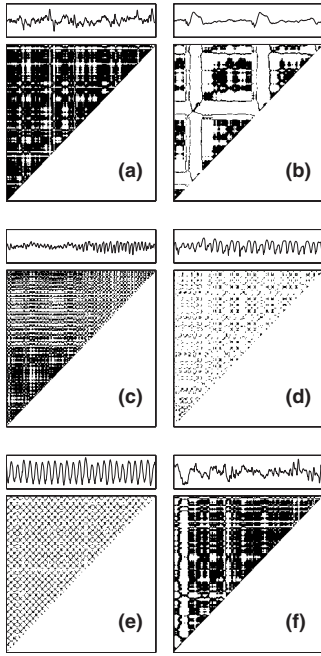


FIG. 2. Each group of two panels represents a segment of ECoG approximately 4.17 s in length (top) and the corresponding recurrence plot (below), computed with  $\epsilon=0.03$ . The top two groups are taken from pre-seizure activity, while the middle and bottom left groups are taken from seizure activity. The bottom right group depicts post-seizure activity.

Black regions on the recurrence plot indicate a point pair within a threshold  $\epsilon$ , but the existence of recurrent points alone is insufficient to determine rhythmicity. We see the emergence of regular patterns in the recurrence plots during the seizure as well as an increased presence of diagonal lines, which indicate signal regions which remained recurrent for some time. Both interseizure and postseizure activity appear to be characterized by a higher percentage of recurrent activity but with little regular structure in the recurrence plots as compared to the nonseizure data. As the seizure becomes increasingly rhythmic, the recurrence plot begins to resemble that of a sine wave [Fig. 2(e)]. Computing metrics sensitive to this distinct feature may enable its automated detection without *a priori* knowledge of the specific frequency bands in which to look, subject to some limitations due to method parameters such as window length.

In Fig. 2, the differences between the nonseizure and seizure time periods highlight the difference between a signal recurrence and rhythmicity. Here, recurrence simply indicates that the signal comes, at some time  $t$ , within  $\epsilon$  of a template point occurring earlier in the signal. More generally, recurrence can be defined as occurrences where a signal segment falls within a set of discrete gates around a specific signal template. For instance, this might be defined by  $\|x[t+(i-1)*T_i]-f(i)\| \leq \epsilon$ , for  $i=1, \dots, m$ , where  $x$  is the measured signal,  $f$  is a set of points comprising the template,  $\epsilon$  is a length scale parameter,  $T_i$  defines the spacing of the points in the template, and  $m$  is the number of points in the template. To examine any recurrences that may be in a segment of signal, every piece of signal is used in turn as this signal template, as in Fig. 2. Figure 3 shows a set of signal templates (solid squares) which represent the target signal of

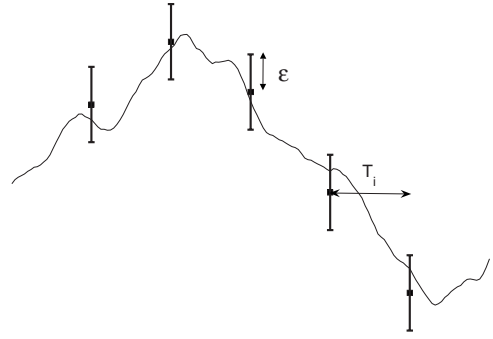


FIG. 3. Recurrence can be defined in terms of occurrences in which a signal passes within  $\epsilon$  of template points spaced by  $T_i$ .

interest as well as the actual measured signal (solid line). If the signal falls within  $\epsilon$  for all the signal templates, as is represented by the brackets, then the signal is recurrent with the template.

In the simpler case shown in Fig. 2, each point within a signal window is used for as a template for every other point occurring later in time, and  $m=1$ . We do not use higher-dimensional delay embedding of the time series in generating Fig. 2 because we are introducing a pattern-matching perspective on recurrence analysis rather than the traditional nonlinear dynamics perspective. Our approach in this paper is to begin with the  $m=1$  case and then gradually increase complexity to illustrate how the technique can be used to capture effects that are traditionally recorded through the time-consuming process of expert visual analysis. In both the general case and the specific case of  $m=1$  many apparent recurrences will be detected if  $\epsilon$  is sufficiently large or if the pattern occurs frequently enough. This is not sufficient to determine whether a signal is rhythmic, which additionally requires regular structure in the recurrence plot, to indicate that recurrences occur in some regular or predictable fashion.

### III. ANALYSIS OF RHYTHMIC TEST PATTERNS

We define rhythmicity in a signal to be a regularly recurring waveform pattern that may be modulated in amplitude, frequency, or temporal spacing by a function that does not vary significantly over any time scale shorter than the rhythmic pattern block. Let  $Q(A, T_Q)$  be a block of signal of amplitude  $A$  and length  $T_Q$  containing the repeated pattern, and let  $R_i(T_R)$  be blocks of arbitrary signal of fixed length  $T_R$ . We then define a rhythmic signal,

$$x_R = [Q(A, T_Q)R_1(T_R)Q(A, T_Q)R_2(T_R) \cdots Q(A, T_Q)R_N(T_R)], \quad (3)$$

where  $R_i \neq R_j$ . The amplitude ( $A$ ), length ( $T_Q$ ) or temporal spacing ( $T_R$ ) may be functions  $A(t)$ ,  $T_Q(t)$ , and  $T_R(t)$ , respectively, provided that  $F(t) - F(t+T_Q) < \epsilon$ , where  $F$  is one of the three above functions and  $\epsilon$  is small. The temporal spacing  $T_R$  may be zero, in which case the rhythmic pattern blocks are not interrupted by other signals.

To test measures developed to characterize rhythmicity, we developed the following set of test segments that incorporate the defined features above:

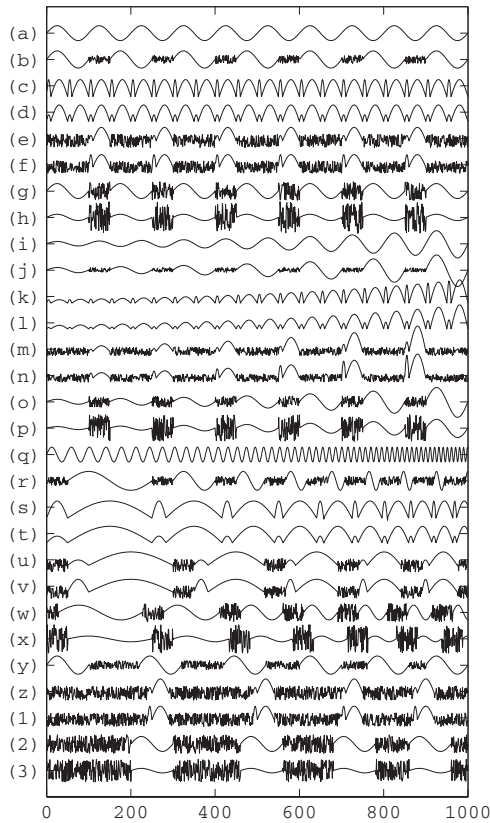


FIG. 4. Simulated rhythmic signal segments 1000 points in length are used to test the rhythmicity algorithm. Segments (a)–(h) are repetitions of signal blocks resembling types of activity commonly seen in seizures. These baseline rhythmic segments are modulated in amplitude [segments (i)–(p)], frequency-chirped [segments (q)–(x)], and varied in temporal spacing [segments (y)–(3)].

- (1) Sine wave of frequency  $f_1$  [Fig. 4(a)].
- (2) Single oscillations of a sine wave of frequency  $f_1$  separated by intervals of random activity of length  $t_1$ , where the random activity is modeled by uniform random noise between  $-0.5$  and  $0.5$  such that the amplitude of the sine wave is approximately *twice* the amplitude of the noise [Fig. 4(b)].
- (3) Single oscillations of a sine wave of frequency  $f_1$  separated by intervals of random activity of length  $t_1$ , where the amplitude of the sine wave is approximately *equal* to the amplitude of the uniform random noise [Fig. 4(g)].
- (4) Single oscillations of a sine wave of frequency  $f_1$  separated by intervals of random activity of length  $t_1$ , where the amplitude of the sine wave is approximately *five times less* than the amplitude of the noise [Fig. 4(h)].
- (5) Repetitions of half-waves of a sine wave of frequency  $f_1$  followed by half-waves of a sine wave of frequency  $f_2$ , where the amplitudes of the two sine waves are *identical* [Fig. 4(c)].
- (6) Repetitions of half-waves of a sine wave of frequency  $f_1$  followed by half-waves of a sine wave of frequency  $f_2$ , where the amplitudes of the two sine waves are *nonidentical* [Fig. 4(d)].
- (7) A pattern block consisting of a half-wave of a sine wave of frequency  $f_1$  followed by a half-wave of a sine wave of frequency  $f_2$  separated by intervals of arbitrary ran-

dom activity of length  $t_1$ , where the amplitudes of the two sine waves are *identical* and the amplitude of the uniform random noise is approximately half that of the signal [Fig. 4(f)].

- (8) A pattern block consisting of a half-wave of a sine wave of frequency  $f_1$  followed by a half-wave of a sine wave of frequency  $f_2$  separated by intervals of arbitrary random activity of length  $t_1$ , where the amplitudes of the two sine waves are *nonidentical* [Fig. 4(e)].

Further patterns are formed by modulating each of these base patterns in amplitude, frequency, or temporal spacing.

Test patterns are depicted in Fig. 4. Figure 4 (a–h) depicts the base patterns while the remaining figures show the base patterns modified by amplitude modulation [Fig. 4 (i–p)], frequency chirping [Fig. 4 (q–x)], and changes in temporal spacing [Fig. 4 (y–3)]. To characterize rhythmicity in these test segments, we examine the distribution of recurrence times. To enable the method to detect recurrent waveforms, as opposed to detecting merely recurrent voltage levels in a signal, we delay embed the signal using the techniques of time-delay embedding,

$$\mathbf{x}_i = \{x_i, x_{i+\tau}, \dots, x_{i+(m-1)\tau}\}, \quad (4)$$

where  $m$  is the embedding dimension and  $\tau$  is a delay time. These parameters are equivalent to the number of points in the template and the spacing between points in the template, respectively, as previously described. Time-delay embedding transforms the scalar time series into a vector time series where each time index contains a small segment of signal of length  $m$ , downsampled by  $\tau$ . Recurrences then become recurrences of this small signal segment.

Embedding parameters  $m$  and  $\tau$  traditionally have been determined through a number of heuristic approaches.<sup>30</sup> However, ECoG data is highly nonstationary and extremely high-dimensional both for seizure and nonseizure data,<sup>20–22,24</sup> making embeddings found using conventional approaches both impractical and arbitrary. We therefore take a pragmatic stance and limit ourselves to parameter choices that are small as possible but sufficient to detect the activity of interest.

Regarding choice of the embedding dimension parameter, for instance, we are particularly interested in approaches that can adequately detect the occurrence of rhythmic signals using embedding dimensions of up to three. Although one can clearly determine recurrent patterns with greater specificity through the use of higher embedding dimensions than typically used in this work, our main interest is on the development of algorithms to detect rhythmic patterns in real time and with minimal computational complexity and high memory efficiency.

We then define the recurrence time for these signal segments,

$$R_{ij}^t = i - j, \quad (5)$$

if  $R_{ij} = 1$ , where  $R_{ij}$  is defined as in Eq. (1). The quantity  $R_{ij}^t$  is not defined when  $R = 0$ , but in practice it is set to a numerical flag, such as  $-1$ . A vector of first return times  $R^t$  is determined by scanning each row of  $R_{ij}^t$  for the first non-negative value where  $j > i + T$ . The quantity  $T$  is a parameter

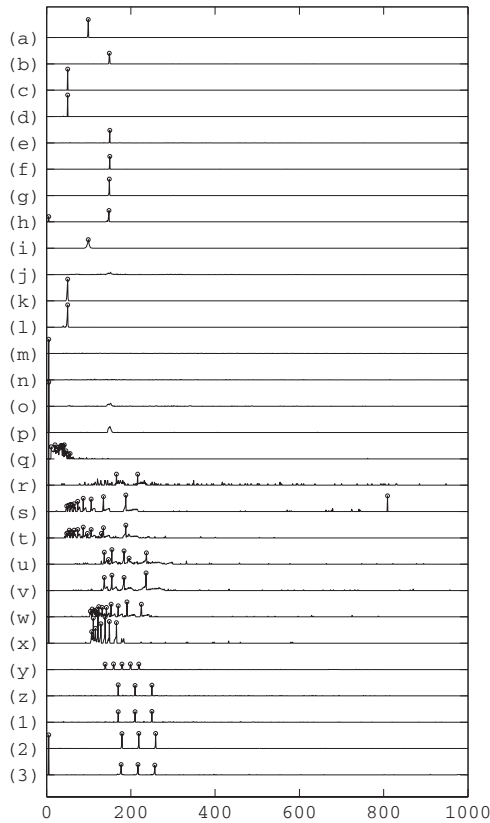


FIG. 5. For the simulated data segments depicted in Fig. 4, the first return times are depicted, with the major peaks indicated by a circle. Prior to analysis, all segments are normalized to zero mean and unit variance. For all segments,  $\epsilon=0.1$ ,  $m=3$ , and  $\tau=5$ .

equivalent to several multiples of the autocorrelation time, to remove trivial recurrences due to autocorrelations. We then compute a histogram of the first return times  $R^i$ , using  $M = e^{0.626+0.4 \ln(N-1)}$  bins, where  $N$  is the number of points in a window, the optimum number of bins in a histogram.<sup>31</sup>

Figure 5 shows the distribution of first return times for each of the test patterns. In the absence of attenuation or chirping, recurrences on the base patterns show a very clear indication of the fundamental timescale for recurrence. Slow amplitude variation, as shown in Fig. 5 (i–p), typically has little effect on the ability to recover these fundamental time scales, though in segments (m) and (n), no recurrent peaks were detected. Frequency chirping, as shown in Fig. 5 (q–x), creates a cluster of peaks around this fundamental time scale and dependent on the severity of the chirps. Finally, for varying lengths of arbitrary signal interrupting patterns, we see one peak for every nearest neighbor pair of individual waveforms. Based on this, we define three metrics to quantify the characteristics of recurrences in the test patterns: (1) The mean of the first recurrence times ( $\bar{R}_i$ ); (2) the variance in the first recurrence times [ $\sigma(R_i)$ ]; and (3) the percent time spent in recurrence  $p_R$ , defined as the ratio of the time spent inside a peak to total time. Table I shows the results of these metrics for the segments depicted in Fig. 4.

Perfect rhythmic repetitions [Fig. 4 (a–h)] result in mean first return times that very accurately match the lengths of the repeated signal rhythmic pattern blocks. Segments showing pure repetitions with no interspersed noise show values

TABLE I. For the rhythmic simulated data segments, this table shows the results of three metrics applied to the first return analysis: The mean of the first return times ( $\bar{R}_i$ ), their variance [ $\sigma(R_i)$ ], and the percent time spent in recurrence  $p_R$ .

Segment	mean( $R_i$ )	var( $R_i$ )	% recurrent
(a)	99	0	1
(b)	149	0	0.65
(c)	50	0	0.96
(d)	50	0	0.98
(e)	150	0	0.24
(f)	150	0	0.25
(g)	149	0	0.65
(h)	148	0	0.53
(i)	99	0	0.45
(j)	149.5	3.5	0.26
(k)	50	0	0.35
(l)	50	0	0.43
(m)	N/A	N/A	0
(n)	N/A	N/A	0
(o)	150	2.8	0.28
(p)	150	1.4	0.32
(q)	37.7	11.1	0.49
(r)	191	35.4	0.02
(s)	152.9	221.7	0.32
(t)	88.6	41.8	0.37
(u)	176	37.4	0.27
(v)	178	43.2	0.23
(w)	141.3	37.3	0.27
(x)	129.9	20.3	0.29
(y)	179	31.6	0.56
(z)	210	40	0.15
(1)	210	40	0.16
(2)	219	40	0.35
(3)	217	40	0.20

of  $p_R$  that are equal to or nearly 1 [Figs. 4(a), 4(c), and 4(d)]. Segments in Figs. 4(b), 4(e), and 4(f) have a  $p_R$  that is slightly less than the fraction of the time spent in rhythmic signal. This agreement with the fraction of time spent in rhythmic signal generally deteriorates as the noise amplitude grows with respect to the rhythmic signal, and in the presence of chirping or amplitude modulation.

No rhythmic activity was detected in segments Fig. 4 (m–n) due to the high degree of amplitude modulation and the relatively small number of rhythmic pattern blocks present in the segment. A larger value for  $\epsilon$  can capture this activity. Additionally, analysis rhythmic pattern blocks that occur only infrequently may benefit from larger time windows so that more examples of the pattern can be captured.

#### IV. RESULTS ON ECG DATA

We analyze 25 ten-minute segments of ECoG, comprising five typical seizures from each of five patients, beginning 5 min before automated seizure detection. Four ECoG segments are shown in Fig. 6 (left) that contain significant rhythmicities. First return times are shown on the corresponding panels on the right-hand side. Recurrences were computed on 1000 point ECoG segments, sampled at 239.75 Hz, representing approximately 4.2 s of data. Seg-

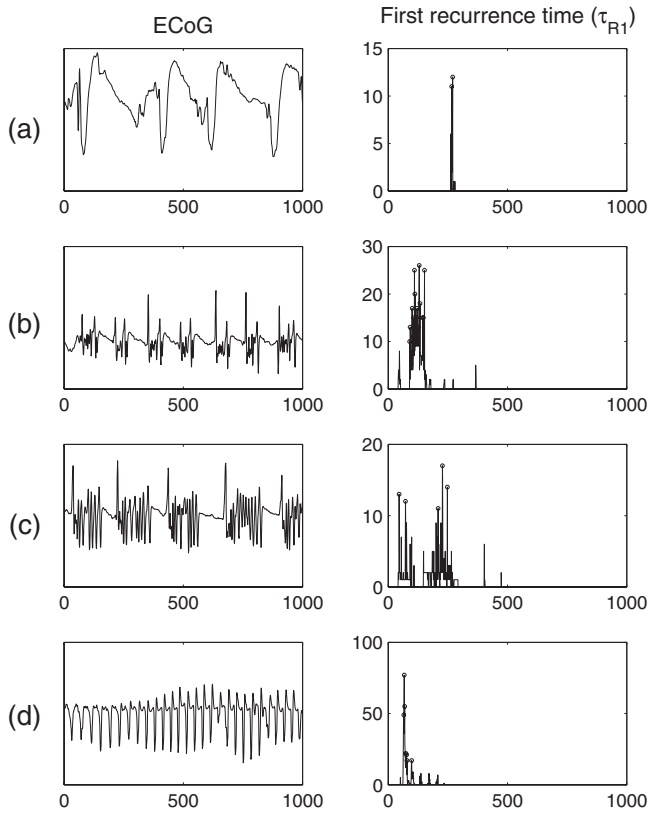


FIG. 6. Typical rhythmic segments of ECoG from the primary seizure onset channel, taken during a seizure. Segments shown are taken from different time intervals in the seizures of two patients. Corresponding times of first recurrences are shown on the right, next to each ECoG segment. Peaks indicated by circles represent the dominant first return times uncovered in the segment.

ments were normalized to unit variance, and delay embedded with an embedding dimension of 3 and a delay time equal to the time at which the signal’s autocorrelation function falls off from the first maximum by 2/3, a typical delay time choice.<sup>32</sup>

Recurrences were computed with length scale  $\epsilon=0.5$ , and  $T=5$ . Segments shown are representative of ECoG during seizure or precursor activity. The extremely rhythmic behavior in segment (d) shows additional peaks beyond the first recurrence, that appear to be multiples of the first. These peaks represent recurrences that were missed on the first returns. Some recurrent periods show a multimodal (often bimodal) distribution, such as segment (c), indicating the presence of recurrences on two different time scales.

To examine how the distribution of recurrence times changes over the course of a seizure, we segment ECoG data into 4 s windows overlapped by 2 s and follow the same procedure described above. Peaks are located using a simple extrema detector that looks for peaks above an amplitude threshold to detect peaks above the noise level.

Figures 7 and 8 depict first return analysis results for two typical ECoG segments containing seizures starting at approximately 18 and 26 s, respectively. For both seizures, mean recurrence times are approximately 50 points (0.21 s) at seizure onset, increasing to approximately 300–350 points (1.25–1.46 s) by the end of the seizure. The seizure in Fig. 7 shows a region of fast rhythmic activity between 18 and 46 s, followed by a relatively sharp transition to slower ac-

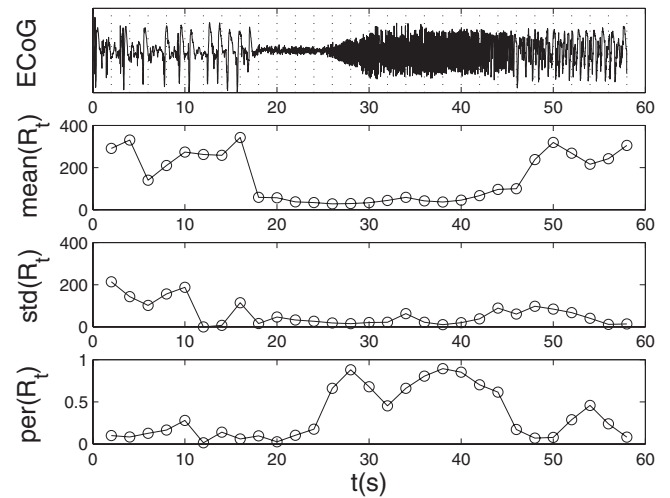


FIG. 7. Using 4 s sliding windows overlapped by 50%, the values of first return statistics (the mean first recurrence time, its standard deviation, and the percent time spent in recurrence) are plotted against the midpoint of the window, indicated by the dashed line on the ECoG plot in the top panel. Windows for which no recurrences were found do not have statistics computed and for these regions, the second through fourth panels are blank.

tivity. The seizure shown in Fig. 8 experiences a more gradual slowing of seizure activity. The fourth panels in Figs. 7 and 8 depict the percentage of time in each window spent in detectable rhythmic behavior. For both seizures, the greatest percentage time spent in rhythmic behavior is near the beginning of the seizure, though it may be that the method preferentially detects rhythmic activity on time scales that are small in comparison to the length of the window.

### V. DISCUSSION

The intent of this paper is to propose a quantitative definition of rhythmicity, a signal feature that has been treated qualitatively, and a set of statistics for characterizing this property. Temporal recurrences, based on repetitions of specific pattern blocks, seem to provide different information than traditional spectral measures. Spectral measures are well-suited for signals with easily-identifiable signatures in

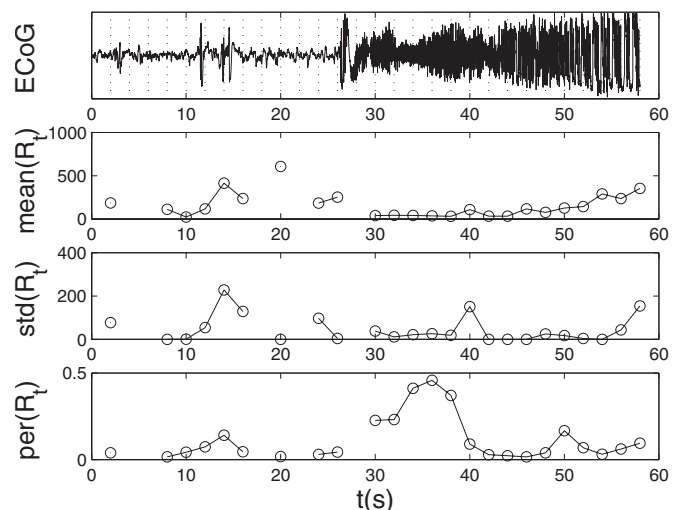


FIG. 8. As in Fig. 7, but with a seizure from a different patient.

the frequency domain. Conversely, temporal recurrences are useful in the time domain for detections of patterns which may have a much more complicated frequency domain representation, due to compound morphologies and nonperiodic repetitions. For complicated signals, recurrence analysis provides a convenient and complementary measure to spectral characteristics that can be used either as a sole analysis or to augment existing seizure detection or prediction algorithms. The recurrent patterns identified by this and others' methods depend upon the threshold choices and the corresponding time and length scales which focus the pattern search. Choice of optimum parameter values for a particular application typically requires some experimentation.

Analysis of recurrent points was originally designed specifically for analysis of nonstationary time series,<sup>2</sup> suggesting that methods based on recurrences may be suitable for analysis of EEG or ECoG. The method proposed in this paper for analysis of seizure rhythmicity uses an approach related to one previously proposed for detection in time series of unstable period orbits (UPOs).<sup>10</sup> UPOs are dynamically unstable periodicities found in chaotic systems, which provide the structure for a chaotic attractor. In their method, the times of first recurrences are computed and the resulting distribution is examined for regularly-spaced peaks with logarithmic scaling.<sup>33</sup> The time scale of the first recurrence is taken to be due to unstable period-one orbits, and peaks at integer multiples are due to period-two, three, or higher orbits. It has been shown that the method also works for transient chaotic time series,<sup>11,12</sup> suggesting that the method may be useful for certain nonstationary signals since transience implies nonstationarity. Thus, it may be possible to detect UPOs, if present, in electrical brain activity using these methods.

Indeed, applications of the Lathrop–Kostelich or alternate UPO detection methods to ECoG may lead one to conclude that seizure data does contain UPOs, and therefore is activity derived from a low-dimensional, chaotic system. This conclusion is attractive, especially in light of two important observations: (1) neuronal hypersynchronization is generally-accepted as an explanation for epileptic seizures and their associated electrographic phenomena,<sup>34</sup> and (2) changes in unstable periodic orbits are associated with synchronization onset in dynamical systems.<sup>35</sup> We might then argue that since neuronal synchrony drives seizures and since synchrony is associated with the alternation of UPOs, then detection of UPO changes in ECoG time series uncovers information about this synchrony and therefore the underlying nonlinear dynamics of this system. While this conclusion is tempting, we find that small segments of completely arbitrary rhythmic signals, especially under conditions of noise, slight attenuation, or frequency chirping, show similar features in first return analysis as UPOs. Thus, the presence of a positive indicator on a first returnlike test for UPOs may be a necessary, but not a sufficient, condition that UPOs exist. This is an important fact to keep in mind when interpreting these analyses on real-world data.

The study of repetitive patterns found in complex signals has obvious practical value regardless of whether their presence is due to chaos, UPOs, or not. If a given signal pattern or feature were never to reappear, it would be of no use to

understand or attempt to detect or predict. The method described in this paper provides a means for identifying such patterns and may be used as a tool to help better understand seizure dynamics.

## ACKNOWLEDGMENTS

This work was supported by NIH under Grant No. 5R01NS046602-02.

- <sup>1</sup>J. Theiler, S. Eubank, A. Longtin, B. Galdrikian, and J. D. Farmer, *Physica D* **58**, 77 (1992).
- <sup>2</sup>J. P. Eckmann, S. O. Kamphorst, and D. Ruelle, *Europhys. Lett.* **4**, 973 (1987).
- <sup>3</sup>M. C. Casdagli, *Physica D* **108**, 12 (1997).
- <sup>4</sup>J. S. Iwanski and E. Bradley, *Chaos* **8**, 861 (1998).
- <sup>5</sup>J. B. Gao, *Phys. Rev. Lett.* **83**, 3178 (1999).
- <sup>6</sup>C. Rieke, K. Sternickel, R. G. Andrzejak, C. E. Elger, P. David, and K. Lehnertz, *Phys. Rev. Lett.* **88**, 244102 (2002).
- <sup>7</sup>C. Rieke, R. G. Andrzejak, F. Mormann, and K. Lehnertz, *Phys. Rev. E* **69**, 046111 (2004).
- <sup>8</sup>N. Marwan and J. Kurths, *Phys. Lett. A* **336**, 349 (2005).
- <sup>9</sup>A. Facchini, H. Kantz, and E. Tiezzi, *Phys. Rev. E* **72**, 021915 (2005).
- <sup>10</sup>D. P. Lathrop and E. J. Kostelich, *Phys. Rev. A* **40**, 4028 (1989).
- <sup>11</sup>M. Dhamala, Y.-C. Lai, and E. J. Kostelich, *Phys. Rev. E* **61**, 6485 (2000).
- <sup>12</sup>M. Dhamala, Y.-C. Lai, and E. J. Kostelich, *Phys. Rev. E* **64**, 056207 (2001).
- <sup>13</sup>E. Bradley and R. Mantilla, *Chaos* **12**, 596 (2002).
- <sup>14</sup>E. G. Altmann, E. C. da Silva, and I. L. Caldas, *Chaos* **14**, 975 (2004).
- <sup>15</sup>M. C. Romano, M. Thiel, J. Kurths, and W. von Bloh, *Phys. Lett. A* **330**, 214 (2004).
- <sup>16</sup>M. Thiel, M. C. Romano, P. L. Read, and J. Kurths, *Chaos* **14**, 234 (2004).
- <sup>17</sup>A. Groth, *Phys. Rev. E* **72**, 046220 (2005).
- <sup>18</sup>N. Marwan, N. Wessel, U. Meyerfeldt, A. Schirdewan, and J. Kurths, *Phys. Rev. E* **66**, 026702 (2002).
- <sup>19</sup>The gold standard for analysis of ECoG and EEG recordings is expert visual inspection, and the standard descriptor of electrographic activity refers to visually apparent features. However, many statistics used in automated EEG/ECoG analysis, particularly those derived from nonlinear dynamics, are not easily translated to these visually-apparent features. Consequently, their electrographic relevance can be difficult to determine.
- <sup>20</sup>I. Osorio, M. A. F. Harrison, Y.-C. Lai, and M. G. Frei, *Clin. Neurophysiol.* **18**, 269 (2001).
- <sup>21</sup>Y.-C. Lai, I. Osorio, M. A. F. Harrison, and M. G. Frei, *Phys. Rev. E* **65**, 031921 (2002).
- <sup>22</sup>Y.-C. Lai, M. A. F. Harrison, M. G. Frei, and I. Osorio, *Phys. Rev. Lett.* **91**, 068102 (2003).
- <sup>23</sup>Y.-C. Lai, M. A. F. Harrison, M. G. Frei, and I. Osorio, *Chaos* **14**, 630 (2004).
- <sup>24</sup>M. A. F. Harrison, I. Osorio, M. G. Frei, S. Asuri, and Y.-C. Lai, *Chaos* **15**, 033106 (2005).
- <sup>25</sup>P. Grassberger and I. Procaccia, *Physica D* **9**, 189 (1983).
- <sup>26</sup>M. C. R. Blasco, Ph.D. thesis, Universitat Potsdam (2004).
- <sup>27</sup>N. Marwan, M. C. Romano, M. Thiel, and J. Kurths, *Phys. Rep.* **438**, 237 (2007).
- <sup>28</sup>I. Osorio, M. G. Frei, and S. B. Wilkinson, *Epilepsia* **39**, 615 (1998).
- <sup>29</sup>This is sufficiently long to capture several repetitions of waveform patterns commonly seen at seizure onset, but short enough to be computationally tractable and enable rapid detection.
- <sup>30</sup>L. M. Pecora, L. Moniz, J. Nichols, and T. L. Carroll, *Chaos* **17**, 013110 (2007).
- <sup>31</sup>R. Otnes and L. Enochson, *Digital Time Series Analysis* (Wiley, New York, 1972).
- <sup>32</sup>M. T. Rosenstein, J. J. Collins, and C. J. D. Luca, *Physica D* **73**, 82 (1994).
- <sup>33</sup>Our method for detection of rhythmicity is similar up to this point, but we perform different analyses on the recurrence distribution.
- <sup>34</sup>W. Penfield and H. Jasper, *Electrophysiology and Experimental Epilepsy* (Little Brown, Boston, 1954), Chap. Epilepsy and the Functional Anatomy of the Brain, pp. 193, 232.
- <sup>35</sup>E. Sander, E. Barreto, K. Josic, C. Morales, and P. So, *Chaos* **13**, 151 (2003).